STUDIES OF InSe AND GaSe LAYERED CRYSTALS INTERCALATED IN IODINE VAPOR

Z.D. KOVALYUK, V.Y. DUPLAVYY, M.M. PYRLJA, V.V. NETYAGA, O.M. SYDOR

I.M. Frantsevych Institute for Problems of Materials Science, Chernivtsi Subdivision, Nat. Acad. of Sci. of Ukraine
(5, Iryna Vilde Str., Chernivtsi 58001, Ukraine; e-mail: chimps@ukrpost.ua)

PACS 73.40.-Lq, 71.35.-y, 78.20.-e, 78.66-w

Iodine intercalates of InSe and GaSe layered single crystals have been obtained. Excitonic transmission spectra are studied for insertion compounds ⟨I⟩GaSe and ⟨I⟩InSe at a temperature of 77 K. In the course of iodine absorption, the energy position of the excitonic maximum is found to shift and the half-width of the excitonic band to vary. For ⟨I⟩GaSe, both changes are found to be nonmonotonous. The frequency dependences of the impedance have been measured for ⟨I⟩GaSe intercalates, and the corresponding equivalent circuit has been proposed. An isotype heterojunction on the basis of ⟨I⟩GaSe is fabricated, and its current–voltage and capacitance–voltage characteristics, as well as the spectral dependences of the quantum efficiency of a phototransducer, are measured.

1. Introduction

Layered crystals of the type A^3B^6, typical representatives of which are gallium and indium monoselenides, become a matter of close attention of scientists, since they are substances promising for use in many branches. The presence of the weak van der Waals coupling between layers makes it possible to produce various intercalation compounds on the basis of GaSe and InSe. Moreover, atoms, ions, or molecules can be introduced in this case, depending on the selected method for intercalating the initial matrix of layered crystal [1–6]. In work [7], results were reported concerning the capability of electrochemical intercalation of GaSe and InSe layered crystals with an electronegative element, iodine, and the determination of changes in electrochemical, electrokinetic, and optical properties of initial crystalline matrices owing to the introduction of the given intercalant. It is of interest to study the process of iodine vapor influence (sorption) in a closed volume on GaSe and InSe properties, which can be of both academic interest and practical applications, in particular, semiconducting materials with prescribed properties and electrodes for secondary power sources [8].

2. Experimental Technique

GaSe and InSe specimens were grown up using the Bridgman method. The sorption of iodine molecules by GaSe and InSe single crystals ($10 \times 5 \times 2$ mm^3 in dimension) was carried out in a closed glass (quartz) vessel. Here, crystalline iodine and GaSe (InSe) crystals were kept at room temperature, which enabled iodine atoms to be introduced into the single-crystalline matrix owing to the action of the iodine vapor pressure. The process was continued for 1–6 weeks in the GaSe case and for 1–3 weeks in the InSe case. The transmission spectra of GaSe and InSe specimens intercalated with iodine were studied.

We also studied the ac properties of ⟨I⟩GaSe and analyzed a possibility to create rectifying structures on its basis. The transmission spectra of crystals were measured on a spectrometer installation developed on the basis of a modified IKS-31 spectrometer. The light propagation direction was perpendicular to the base plane of the crystal. The device resolution in the spectral interval $2.095-2.14$ meV was $0.6-1.2$ meV (diffraction gratings with 1200 and 600 line/mm, respectively, were used).

The usage of a UTRECS-RTR cryostat system gave us an opportunity to study the transmission spectra at a temperature of 77 K. The specimen temperature was monitored with the help of a TPK-1.1 germanium resistance thermometer; the corresponding accuracy of specimen temperature stabilization was 0.5 K.

We have studied the dependence of the spectral position and the half-width of the excitonic maximum in the ⟨I⟩GaSe and ⟨I⟩InSe compounds on the iodine sorption duration at 77 K. For ⟨I⟩GaSe, we studied the temperature dependences of current-voltage characteristics (IVCs) in the range $243 - 290$ K and the capacity-voltage characteristics (CVCs) at frequencies of 100, 250, and 500 kHz. The impedance properties of ⟨I⟩GaSe specimens were measured before and after their intercalation in iodine vapors, in the frequency range $10^{-1} \div 10^4$ Hz, at room temperature, and using the impedance spectroscopy method. Measurements

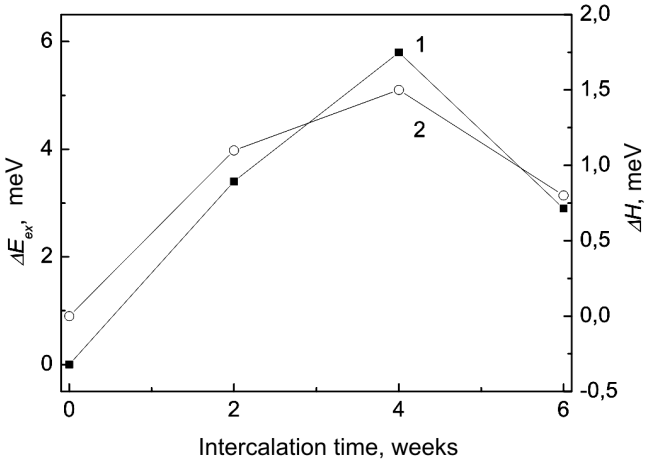

Fig. 1. Dependences of the excitonic maximum energy position shift $\Delta E_{\rm ex}$ (*1*) and the excitonic band half-width ΔH (*2*) on the intercalation time for ⟨I⟩GaSe compound at T=77 K

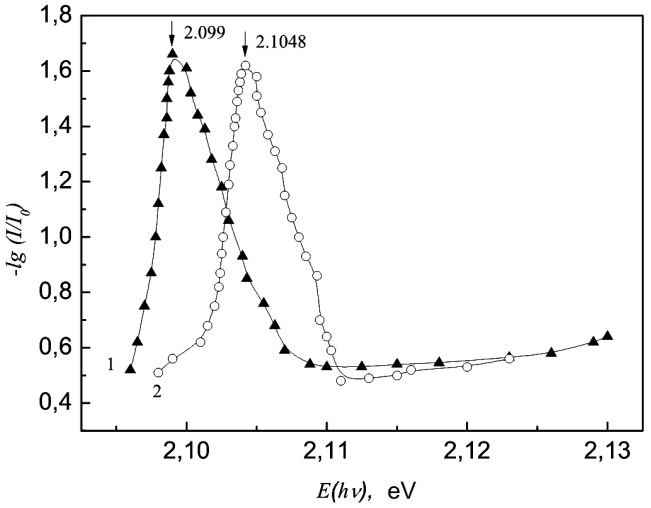

Fig. 2. Optical density spectra of initial GaSe (*1*) and ⟨I⟩GaSe intercalated for 4 weeks (*2*) at T=77 K

were carried out on a combined installation composed of Solartron 1255 FRA and Solartron 1286 modules. The amplitude of a sinusoidal signal was 300 mV. The frequency dependence of the complex impedance was analyzed using the grapho-analytical method with the help of the Zview 3.1 software package (Scribner Associates).

3. Results and Their Discussion

3.1. Exciton transmission spectra of ⟨I⟩GaSe and ⟨I⟩InSe

The dependences of the energy position shift of the exciton maximum ($\Delta E_{\rm ex}$) and the exciton band half-width increase (ΔH) for iodine intercalant ⟨I⟩GaSe on the intercalation time t are characterized by a nonmonotonous behavior at nitrogen temperature (Fig. 1). When GaSe specimens were held in iodine vapors, those parameters grew first ($\Delta E_{\rm ex}$ = 3.2 meV and ΔH = 1.2 meV at t = 2 weeks, and $\Delta E_{\rm ex}$ = 5.8 meV and ΔH = 1.5 meV at t = 4 weeks). Then the reverse changes were observed ($\Delta E_{\rm ex}$ = 2.9 meV and ΔH = 0.6 meV at t = 6 weeks). In Fig. 2, the optical density spectra $-\lg(I/I_0)$ versus $h\nu$ measured at T = 77 K for initial GaSe crystal and GaSe crystal subjected to the iodine sorption for four weeks are depicted.

The presented results evidence a shift of the energy position of the exciton maximum toward high energies– from 2.099 eV for initial GaSe to 2.1048 eV for ⟨I⟩GaSe– and a growth of the exciton absorption band half-width

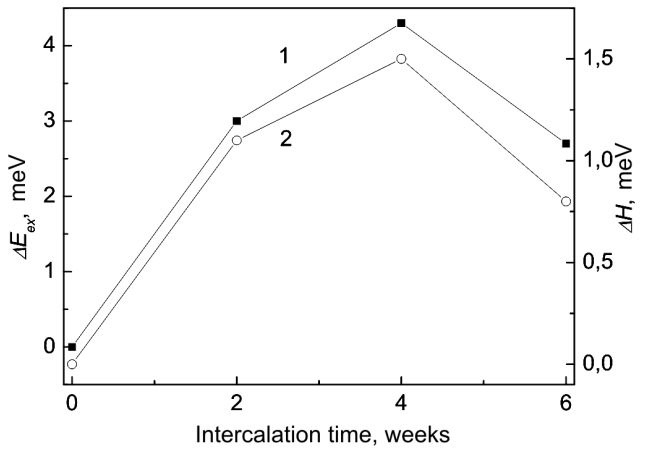

Fig. 3. The same as in Fig. 1, but after holding the intercalated specimen for 21 days in air

ΔH–from 3.6 meV for GaSe to 5.1 meV for ⟨I⟩GaSe (t = 4 weeks).

In Fig. 3, the nonmonotonous dependences $\Delta E_{\rm ex}(t)$ and $\Delta H(t)$ measured at 77 K for ⟨I⟩GaSe specimens held for 21 days in air after the intercalation are exhibited ($\Delta E_{\rm ex}$ = 2.9 meV and ΔH = 1.2 meV at t = 2 weeks, $\Delta E_{\rm ex}$ = 4.1 meV and ΔH = 1.4 meV at t = 4 weeks, and $\Delta E_{\rm ex}$ = 2.6 meV and ΔH = 0.65 meV at t = 6 weeks). The data obtained allowed us to make a conclusion that ⟨I⟩GaSe specimens, being kept for 21 days in air at room temperature after the intercalation, reduced their parameters $\Delta E_{\rm ex}$ and ΔH, approaching

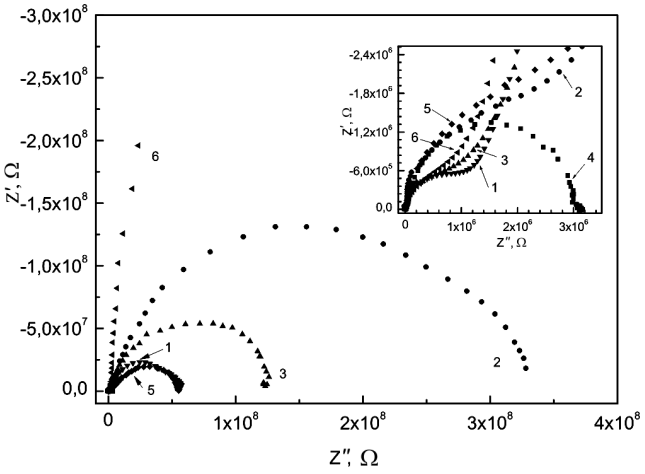

Fig. 4. Frequency dependences of the real, Z', and imaginary, Z'', components of the complex impedance Z^* of specimens in the Nyquist coordinates

the "pure" GaSe state. The results of experimental measurements of the transmission spectra $-\lg(I/I_0)$ versus $h\nu$ for InSe and ⟨I⟩InSe ($t = 2 \div 3$ weeks) at 77 K enabled us to determine the changes of $E_{\rm ex}$ (toward high-energy values) and H that were induced by the iodine sorption (Table 1).

As was marked above, the iodine vapor pressure allowed iodine atoms to be introduced into the crystalline matrix (into the van der Waals gap) of GaSe and InSe, which gave rise to a considerable modification of optical properties of initial crystalline matrices. It is worth noting that the nonmonotonous behavior of $\Delta E_{\rm ex}(t)$ and $\Delta H(t)$ was already observed for hydrogen- [9, 10], alkaline- [11], and alkaline-earth-intercalated [12, 13] GaSe and InSe. The corresponding explanations were put forward on the basis of the ideas concerning the influence of a deformation (in particular, the intercalation) on the energy spectrum reconstruction in a layered crystal. In the general case, a shift $\Delta E_{\rm ex}(t)$ toward the high-energy region was associated with the variation of the energy gap width E_g occurred as a result of interlayer and in-layer distortions which are characterized by different signs of the deformation potential [9–13]. The reverse variation of the dependence $\Delta E_{\rm ex}(t)$ for ⟨I⟩GaSe compound stems from a variety of factors which were specified in works [9–13]. There is a modern explanation for the parameter $\Delta E_{\rm ex}$ change in GaSe and InSe at introducing iodine [14]. The appearance of an iodine atom in the van der Waals gap generates the interlayer pressure. As a result, the interlayer lattice parameter c increases with the intercalation time. In our case, when ⟨I⟩GaSe and ⟨I⟩InSe compounds were obtained following the sorption method, as well as in works [10, 14], a shift of the exciton maximum $\Delta E_{\rm ex}$ at 77 K with growing t may probably originate from an increase of the crystal dielectric constant ε, when iodine appears in the van der Waals gap.

To explain the variation of the parameter ΔH in time t, the following circumstance should be taken into consideration. When atoms are introduced into the crystal, then, owing to a chaotic arrangement of intercalant atoms, the potential reliefs in intercalates ⟨I⟩GaSe and ⟨I⟩InSe become less periodic than those in initial crystals (it affects the exciton dispersion [15]). The exciton radius decreases at that, which suppresses, to some extent, the processes of fluctuation relief averaging. It is the reasons indicated above that are responsible for a change of ΔH in the course of sorption.

To explain the results of our experimental measurements of the optical spectra of ⟨I⟩GaSe and ⟨I⟩InSe compounds after holding them in air for 21 days (Table 1), the following peculiarity of the anion intercalation into layered crystals is to be noted. It consists in that, when anions, in general, and iodine ions, in particular, are introduced, an electric incompatibility between the initial crystal and the introduced impurity manifests itself. The essence of this incompatibility is as follows. Since the structure of layered A^3B^6 crystals looks like a stack of nanolayers (–BAAB–BAAB–), with the stack being oriented along the **c**-axis of the hexagonal lattice, chalcogene atoms that are located along the edges of every nanolayer slightly attract the electron cloud to create a certain negative charge distributed along the van der Waals gap. Therefore, iodine atoms, when penetrating into the interlayer space of the crystal, cannot form a stable bond with the matrix and try either to leave the crystal or to fix themselves at charged defects of the crystal structure of a specimen. The incompatibility between the intercalant and the matrix results in that a certain deintercalation is observed, provided that no new ions are supplied.

T a b l e 1. Changes of the excitonic maximum energy position $\Delta E_{\rm ex}$ and the excitonic band half-width ΔH for ⟨I⟩InSe

Intercalation time	$\Delta E_{\rm ex}$, meV	ΔH, meV
pure InSe	1.3275	3.8
⟨I⟩InSe, $t = 2$ weeks	1.3305	4.6
⟨I⟩InSe, $t = 3$ weeks	1.3283	5.1

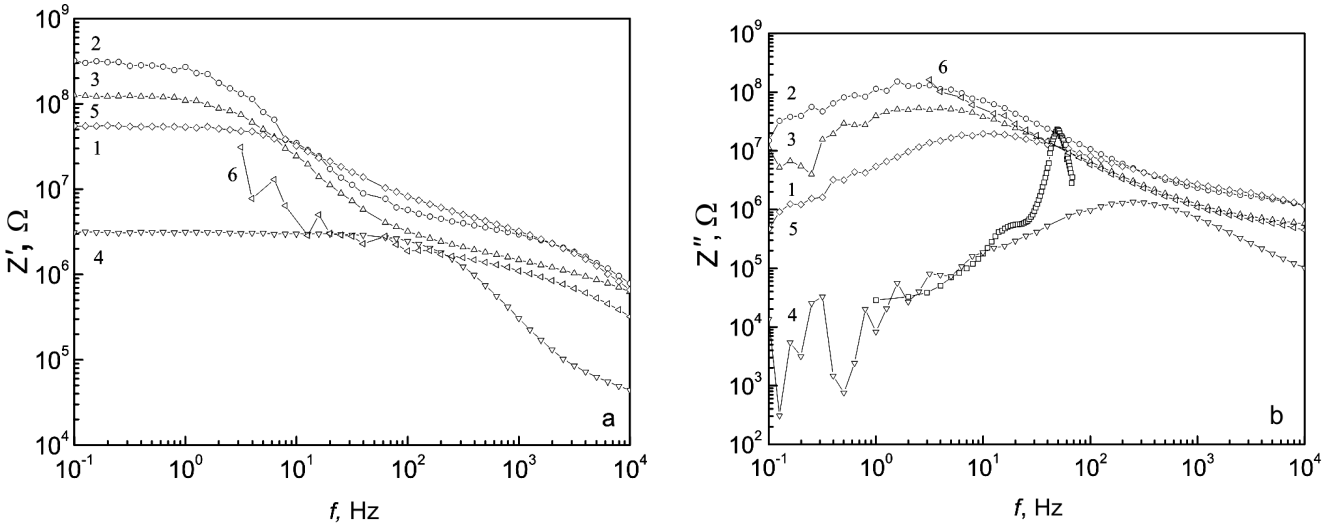

Fig. 5. Frequency dependences of the real, Z' (*a*), and imaginary, Z'' (*b*), components of the impedance of non-intercalated GaSe (*1*) and $GaSeI_x$ intercalated with iodine for 1 (*2*), 2 (*3*), 3 (*4*), 4 (*5*), and 5 weeks (*6*)

3.2. Researches of ⟨I⟩GaSe impedance

In the frequency dependences of the real and imaginary impedance components, two linear sections with different slope angles and a transient section are observed in the studied frequency range. Such a situation takes place for both the initial GaSe specimen and all ⟨I⟩GaSe specimens intercalated for different times. A transition from the first to the second dispersion sections corresponds to the maximum in the frequency dependence of the imaginary component $\mathrm{Im}(z)$ of the complex impedance (Fig. 5). The sections are connected in parallel in an equivalent circuit, and each section corresponds to an individual dispersion process (Fig. 6). In Fig. 6, CPE1 is a constant phase element, the impedance of which corresponds to the following expression:

$$Z_{\mathrm{CPE}} = 1/[Y_0(j\omega)^n], \tag{1}$$

where Y_0 is a frequency-dependent factor, and n is a power exponent that governs the character of the impedance frequency dependence. At $n = 1$ and 0, the element CPE transforms into ordinary elements with lumped RCL-parameters. At $n < 1$, it describes a frequency-dependent lumped element $C(\omega)$. When developing this model, we took into consideration that both contacts are symmetric, and the model structure consists, therefore, of two major components: the impedance of a bulk material and the impedance of contact barriers which are responsible for two semicircles in the Nyquist diagram (Fig. 4) in the high- (in the inset) and low-frequency regions, respectively.

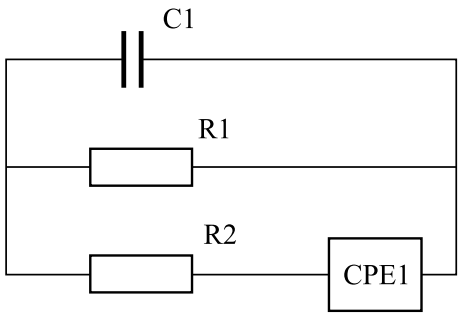

Fig. 6. Equivalent circuit

Proceeding from the basic principle of the impedance simulation, which reduces the analysis to the flux (current) simulation, the physical content of the model was interpreted as an image of simultaneous parallel phenomena. In the frequency range 0.1–100 Hz, the dispersion process corresponds to the near-contact barrier capacities with the curve slope of about 0. Accordingly, it can be presented as a parallel connection of capacitance $C1$ and resistance $R1$ which reflect the influence of a parasitic capacitance (between two planes of the measuring electrodes) and a resistance corresponding to the bulk electronic conductivity, respectively. The second section at frequencies 10^2–10^4 Hz corresponds to a electroneutral specimen volume. It has different slope angles at different intercalation times; accordingly, its equivalent circuit consists of dispersion capacitance CPE1 and resistance $R2$ which take the inhomogeneity of the intercalant distribution during the intercalation into ac-

T a b l e 2. Variations of equivalent scheme element parameters during intercalation

Intercalation time	$R1$, Ω	$C1$, F	Y_0, cm · s	n	$R2$, Ω
pure GaSe	5.7609×10^7	1.569×10^{-17}	2.5858×10^{-11}	0.9263	17544
1 week	3.2143×10^8	8.72×10^{-18}	1.8742×10^{-11}	0.94017	12455
2 weeks	1.3275×10^8	7.437×10^{-17}	4.6574×10^{-11}	0.87874	10765
3 weeks	3.069×10^6	3.849×10^{-11}	5.1312×10^{-12}	1.1	37536
4 weeks	5.8082×10^7	1.0117×10^{-11}	2.1369×10^{-11}	0.92594	0.72874
5weeks	1.6524×10^{19}	2.0416×10^{-12}	1.8615×10^{-10}	0.80975	0.14529

count. The elements CPE1, for which $n \approx 0.5$, simulate an impedance for ideal diffusion, and those, for which $0.5 < n < 1$, an impedance for deformed diffusion. At $0 < n < 0.5$, CPE1 describes the impedance of a pure or distributed resistive element. The key impedance parameters for the examined specimens are quoted in Table 2.

Hence, the impedance researches carried out in the frequency range $10^{-1} - 10^4$ Hz testify that no additional mechanisms of charge carrier transport are observed in GaSe specimens intercalated with iodine. The corresponding conductivity changes can be associated with increase in the through conductivity which plays a crucial role in the relaxation process [16, 17]. The frequency dependence of the impedance was used to draw an equivalent circuit which revealed the presence of two different regions: a bulk part of specimens and a barrier part near the contacts. The regions are characterized by different time constants of relaxation processes owing to a probable inhomogeneous distribution of the introduced intercalant.

3.3. Properties of ⟨I⟩GaSe-based heterojunctions

To fabricate an isotype heterojunction ⟨I⟩GaSe–GaSe, the lower part of a GaSe specimen was immersed into liquid-like iodine during the intercalation process. Owing to a specificity of the chosen intercalation technique, a considerable inhomogeneity of the introduced impurity distribution over the crystal volume was observed. For GaSe, it was found that the penetration of the impurity into the matrix layers that were immersed into liquid-like iodine occurred much more intensively than that into the rest semiconductor volume. To confirm it, the upper and lower parts of intercalated crystal were cleaved off.

Hence, if this intercalation technique is used, near-surface layers enriched with iodine are formed. Therefore, the obtained system can be regarded as an isotype homojunction ⟨I⟩GaSe–GaSe. Its inner potential barrier is caused by a shift of the Fermi level in ⟨I⟩GaSe toward the energy gap midpoint (due to the compensation of charge carriers in the semiconductor matrix) in comparison with the Fermi level position in GaSe. For the intercalates obtained, we studied the temperature dependences of current-voltage characteristics (IVCs) in the temperature range $243 - 290$ K, the capacity-voltage characteristics (CVCs) at frequencies of 100, 250, and 500 kHz, and the spectral dependences of a photocurrent. The researches were confined from above by a temperature of 290 K, because of a considerable iodine deintercalation at higher temperatures (the phenomenon of thermally stimulated deintercalation). For intercalated crystals, the structures of intercalated and pure gallium selenides created by the optical contact bonding method [18] were additionally studied.

In Fig. 7, the temperature dependences of forward IVC branches of gallium monoselenide intercalated with iodine (a) and the ⟨I⟩GaSe–GaSe optical contact (b) are exhibited. Both structures revealed pronounced diode properties. For instance, the rectification factor k was about 300 and 1000, respectively, at the bias voltage $V = 2$ V. Figure 7 demonstrates that the initial sections of IVCs at low biases are affected by shunt currents. At voltages $V > 0.1$ V, the slope of linear sections in the dependences for the optical contact ⟨I⟩GaSe–GaSe (Fig. 7,b) changes with temperature, and the diode coefficient $n = 2.4$ determined from those slopes testifies to the existence of a tunnel-recombination component in the charge transfer mechanism. The absence of a similar section in the IVC of iodine-intercalated gallium monoselenide (Fig. 7,a) is evidently associated with a junction "smearing" in the structure. At high current densities, the IVCs deviate from the linear law for both types of structures under consideration, mainly reflecting the charge transfer through the series resistance rather than the actual mechanism of current flow through the potential barrier.

In Fig. 8, the spectral dependence of the relative quantum efficiency of the phototransformation for gallium selenide intercalated with iodine is shown. One should pay attention to the absence of a short-wave decay which is usually related to surface states and an increase in the

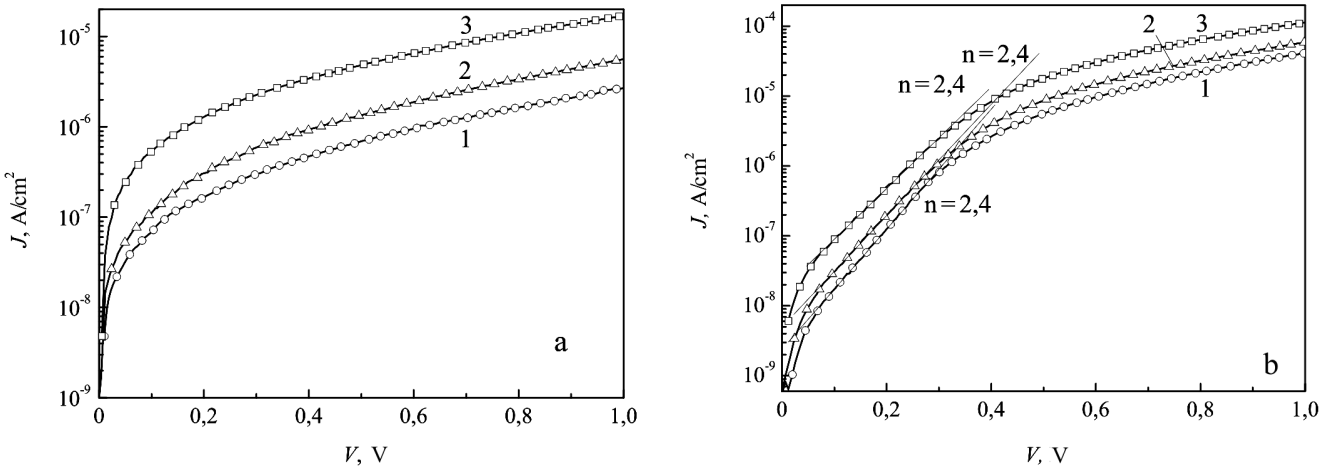

Fig. 7. IVCs of iodine-intercalated gallium selenide (*a*) and the GaSe⟨I⟩–GaSe optical contact (*b*) at various temperatures: T = 243 (*1*), 262 (*2*), and 290 K (*3*)

surface recombination rate [19]. This evidences the inertness and the stability of the semiconductor surface with respect to iodine. At the same time, the behavior of the long-wave photoresponse edge is governed by the following circumstance. The appearance of iodine in the van der Waals gap leads to a nonzero interlayer pressure. As a result, the interlayer lattice parameter grows, which was experimentally observed in researches on the hydrogen intercalation into InSe and GaSe layered crystals [9]. Taking the specificity of the gallium selenide crystalline structure, one can assert that the intercalant stimulates a substantial increase of deformation stresses in the layered crystal. At the same time, the near-band-edge photoresponse peak has to be easily registered in perfect GaSe crystals at room temperature. Instead, in low-quality defect crystals, the fine structure of exciton absorption spectra is not observed, which is characteristic of Fig. 8. Such a confrontation points to the mechanism of processes that take place in gallium selenide layered crystals at the intercalation with iodine.

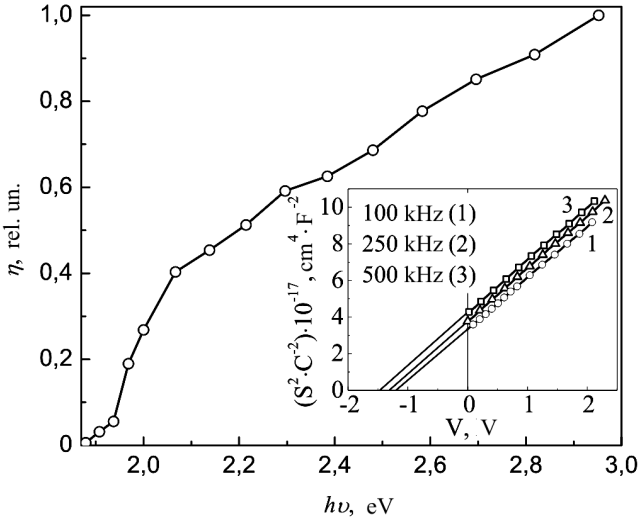

Fig. 8. Spectral dependence of the relative quantum efficiency for the photoconversion in GaSe intercalated with iodine. (inset) CVCs of the optical contact GaSe⟨I⟩–GaSe at various frequencies

To confirm that a potential barrier does exist in the structures concerned, we measured their CVCs. The linearity of frequency CVCs for the optical contact ⟨I⟩GaSe–GaSe testified to a sharp character of the junction formed (see the inset in Fig. 8). The value of built-in potential was determined analogously to work [20] and was found to be about 1.2 eV. For the other type of structures under investigation, a different scenario was observed. The presence of a wide transition region between the iodine-intercalated and non-intercalated parts of GaSe semiconductor distorted the CVC linearity. During a month, the studied structures demonstrated a degradation of their rectification parameters, which is related to the iodine deintercalation. For instance, the parameter k decreased by two orders of magnitude. However, the hermetization of specimens with an epoxy compound allowed us to preserve all the parameters invariable in time.

4. Conclusions

In this work, we have studied GaSe and InSe compounds intercalated in iodine vapors. This intercalation tech-

nique is found applicable to affect physical characteristics of the intercalation matrix. The scheme of ⟨I⟩GaSe intercalate substitution is developed, and changes in the parameters of equivalent circuit elements during the intercalation are examined. A possibility to create isotype heterojunctions on the basis of ⟨I⟩GaSe is analyzed.

1. Z.D. Kovalyuk, T.P Prokipchuk, A.I. Seredyuk, and K.D. Tovstyuk, Fiz. Tverd. Tela **29**, 2191 (1987).
2. V.A. Kulbachinski, M.Z. Kovalyuk, and M.N. Pyrlja, J. Phys. I (Paris) **4**, 975 (1994).
3. Z.D. Kovalyuk, M.N. Pyrlja, A.I. Seredyuk, and K.D. Tovstyuk, Izv. Akad. Nauk SSSR, Neorg..Mater. **21**, 1625 (1985).
4. V.V. Dragomeretskii, Z.D. Kovalyuk, M.N. Pyrlja, A.I. Seredyuk, and K.D. Tovstyuk, Dokl. Akad. Nauk UkrSSR **9**, 77 (1987).
5. S.S. Ishchenko, M.L. Ivaniichuk, D.V. Korbutyak *et al.*, Fiz. Tekh. Poluprovodn. **15**, 2045 (1981).
6. D.V. Korbutyak, L.A. Demchina, V.G. Litovchenko, and Z.D. Kovalyuk, Fiz. Tekh. Poluprovodn. **17**, 814 (1983).
7. V.B. Boledzyuk, Z.D. Kovalyuk, and M.M. Pyrlja, Ukr. Fiz. Zh. **54**, 6 (2009).
8. V.V. Dragomeretskii, Z.D. Kovalyuk, M.N. Pyrlja, A.I. Seredyuk, and K.D. Tovstyuk, Author's certificate 1318124.
9. Z.D. Kovalyuk, M.N. Pyrlja, and V.B. Boledzyuk, Zh. Fiz. Dosl. **6**, 2 (2002).
10. V.B. Boledzyuk, Z.D. Kovalyuk, and M.N. Pyrlja, Alternat. Energet. Ekolog. **31**, 11 (2005).
11. V.K. Lukyanyuk, S.P. Voronyuk, and Z.D. Kovalyuk, Phys. Status Solidi B **30**, 155 (1988).
12. Z.D. Kovalyuk, M.N. Pyrlja, A.I. Seredyuk, and V.I. Vitkovskaya, Izv. Vyssh. Ucheb. Zaved. Fiz. **10**, 51 (1992).
13. V.B. Boledzyuk, Z.D. Kovalyuk, and M.N. Pyrlja, Neorg. Mater. **45**, 11 (2009).
14. Yu.I. Zhirko, Z.D. Kovalyuk, M.M. Pyrlja, and V.B. Boledzyuk, in *Hydrogen Materials Science and Chemistry of Carbon Nanomaterials*, edited by T.N. Veziroglu *et al.* (Kluwer, Dordrecht, 2004), p. 172.
15. V.L. Bonch-Bruevich, I.P. Zvyagin, R. Keiper, A.G. Mironov, R. Enderlein, and B. Esser, *Electron Theory of Disordered Semiconductors* (Nauka, Moscow, 1981) (in Russian).
16. A.K. Jonscher, C. Pickup, and Sh.H. Zaidi, Semicond. Sci. Technol. **1**, 71 (1986).
17. A.K. Jonscher, Solid-State Electron. **33**, 737 (1990).
18. S. Shigetomi and T. Ikari, J. Appl. Phys. **88**, 3 (2000).
19. S.M. Sze, *Physics of Semiconductor Devices* (Wiley, New York, 1981).
20. A.M. Goodman, J. Appl. Phys. **34**, 2 (1963).

Received 21.05.10.
Translated from Ukrainian by O.I. Voitenko

ДОСЛІДЖЕННЯ ШАРУВАТИХ КРИСТАЛІВ GaSe ТА InSe, ІНТЕРКАЛЬОВАНИХ У ПАРАХ ЙОДУ

З.Д. Ковалюк, В.Й. Дуплавий, М.М. Пирля, В.В. Нетяга, О.М. Сидор

Р е з ю м е

Отримано йодні інтеркаляти шаруватих кристалів GaSe та InSe. Для ⟨I⟩GaSe та ⟨I⟩InSe проведено дослідження екситонних спектрів пропускання при 77 K. Встановлено, що в процесі сорбції йоду відбувається зміщення енергетичного положення екситонного максимуму і півширини екситонної смуги, при цьому для ⟨I⟩GaSe зміщення мають немонотонний характер. Для ⟨I⟩GaSe досліджено частотні залежності імпедансу та побудовано еквівалентну схему. На основі ⟨I⟩GaSe створено ізотопний гетероперехід, досліджено вольт-амперні та вольт-фарадні характеристики, а також спектральні залежності квантової ефективності фотоперетворювача.